Design of a Four-Bar Latch Mechanism and a Shear-Based Rotary Viscous Damper for Single-Axis Prosthetic Knees

V. N. Murthy Arelekatti
Global Engineering and Research Lab,
Department of Mechanical Engineering,
Massachusetts Institute of Technology,
Cambridge, MA 02139
e-mail: murthya@mit.edu

Nina T. Petelina[1]
Global Engineering and Research Lab,
Department of Mechanical Engineering,
Massachusetts Institute of Technology,
Cambridge, MA 02139
e-mail: petelina@mit.edu

W. Brett Johnson
Global Engineering and Research Lab,
Department of Mechanical Engineering,
Massachusetts Institute of Technology,
Cambridge, MA 02139
e-mail: wbj@mit.edu

Matthew J. Major
Department of Physical Medicine and Rehabilitation,
Northwestern University,
Chicago, IL 60611
e-mail: matthew-major@northwestern.edu

Amos G. Winter, V
Global Engineering and Research Lab,
Department of Mechanical Engineering,
Massachusetts Institute of Technology,
Cambridge, MA 02139
e-mail: awinter@mit.edu

With over 30 million people worldwide requiring assistive devices, there is a great need for low-cost and high-performance prosthetic technologies that can enable kinematics close to able-bodied gait. Low-income users of prosthetic knees in the developing world repeatedly report the need for n inconspicuous gait to mitigate the severe socioeconomic discrimination associated with disability. However, passive prosthetic knees designed for these users have primarily focused on stability and affordability, often at the cost of the high biomechanical performance that is required to replicate able-bodied kinematics. In this study, we present the design and preliminary testing of two distinct mechanism modules that are novel for passive prosthetic knee applications: the stability module and the damping module. These mechanisms are designed to enable users of single-axis, passive prosthetic knees to walk with close to able-bodied kinematics on level-ground, specifically during the transition from the stance phase to the swing phase of the gait cycle. The stability module was implemented with a latch mounted on a virtual axis of a four-bar linkage, which can be engaged during early stance for stability and disengaged during late stance to initiate knee flexion. The damping module was implemented with a concentric stack of stationary and rotating pairs of plates that shear thin films of high-viscosity silicone oil. The goal of the resulting first-order damping torque was to achieve smooth flexion of the prosthetic knee within the able-bodied gait range (64 ± 6 deg). For preliminary user-centric validation, a prototype prosthetic knee with the stability module and two different dampers (with varying damping coefficients) was tested on a single subject with above-knee amputation in India. The stability module enabled smooth transition from stance to swing with timely initiation of knee flexion. The dampers also performed satisfactorily, as the increase in the damping coefficient was found to decrease the peak knee flexion angle during swing. The applications of the mechanisms presented in this article could significantly improve the kinematic performance of low-cost, passive prosthetic knees. [DOI: 10.1115/1.4052804]

Keywords: bio-inspired design, mechanism design, prosthetics

1 Introduction

According to a recent estimate from the World Health Organization, over 30 million people are in need of prosthetic and orthotic devices across the world [1–3]. Past studies have reported widespread occurrence of lower limb amputation in developing countries, with close to 300,000 persons with above-knee amputation in India, where our research is focused [4–6]. A majority of above-knee amputations in developing countries are carried out due to a multitude of factors such as poor health care, lack of emergency response, unsafe work conditions, traffic accidents, and lifestyle choices [4,7,8]. Past studies have reported that about 50% of persons with amputation in India lose or change their jobs immediately after their injury. The resulting economic deprivation is often exacerbated by the social stigma associated with disability and amputation [9–11]. Individuals with lower limb amputation repeatedly report the need for an inconspicuous gait to mitigate the socioeconomic discrimination that they face, demanding prosthetic performance that can enable kinematics close to able-bodied gait [4,6]. However, only a small number of commercially available prostheses have been designed to enable able-bodied kinematics of walking among low-income prosthesis users [7,8]. Most of the low-cost prostheses designed for the developing world are yet to be adopted at scale due to limitations in their biomechanical performance, mechanical design, manufacturing processes, supply chain, clinical training, and maintenance [4,7,8]. There is thus an urgent need for high-performance, low-cost passive prostheses that can enable kinematics close to able-bodied gait, increase metabolic efficiency for the users, and mitigate socioeconomic discrimination faced by users in the developing world.

In this article, we present the mechanism design and preliminary testing of two distinct modules relevant to single-axis, passive prosthetic knees. The aim of these modules is to enable kinematics close to able-bodied gait for level-ground walking, specifically during the transition from stance phase to swing phase of the gait cycle. This study builds upon our prior research focused on the biomechanical analysis, mechanical design, and user-centric testing of a new passive prosthetic knee for low-income users in developing countries [4,13–19]. This article only concentrates on passive solutions, as active prosthetic knees cost dramatically more than the passive devices provided in developing countries and require power access that might not be available to the user [18]. The first module, called the "stability module," is a novel latch mechanism implemented with a four-bar linkage with the specific function of achieving stability during the early-stance phase and initiating timely knee flexion in preparation for the swing phase. The second module, called the "damping module," is a rotary viscous damper that can provide appropriate flexion control during the

[1]Corresponding author.

Contributed by the Mechanisms and Robotics Committee of ASME for publication in the Journal of Mechanisms and Robotics. Manuscript received January 3, 2021; final manuscript received September 23, 2021; published online November 18, 2021. Assoc. Editor: Chin-Hsing Kuo.

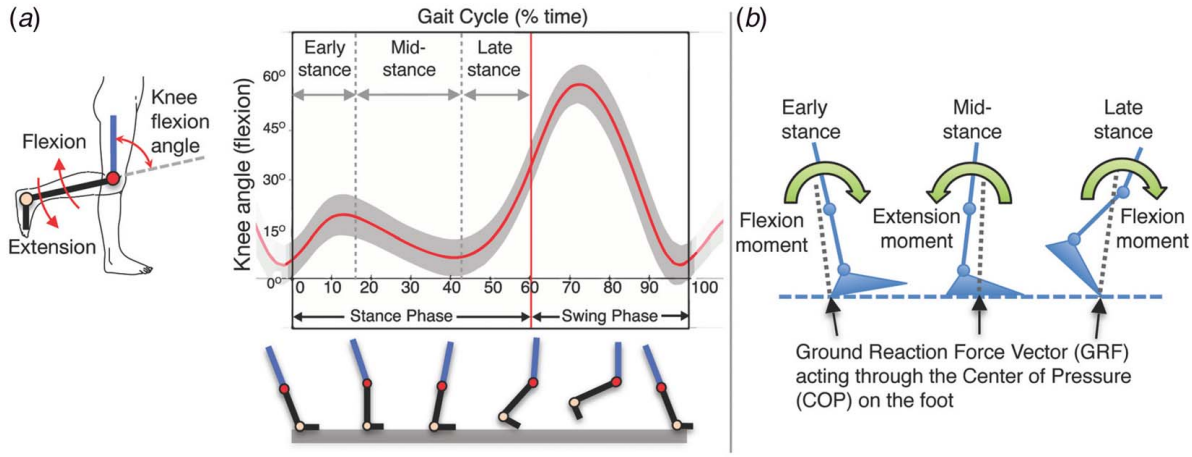

Fig. 1 Able-bodied knee kinematics through the gait cycle. (*a*) Knee angle (red curve) with ±1 standard deviation (SD) shown by the band [12]. The illustration below the horizontal axis shows the corresponding leg orientation through the gait cycle. (*b*) The direction of the moment caused by the GRF changes through the stance phase due to the COP progression and the relative orientation of the leg.

transition from the stance phase to the swing phase. These two mechanism modules offer unique advantages in achieving the desired functions of stability and damping compared to the mechanisms that are currently being used in commercial passive knee prostheses designed for the developing world. In addition, these modules involve novel implementation of mechanisms that can be readily integrated into the architecture of existing single-axis prosthetic knee units without major mechanical alterations.

This article is organized in three sections. First, we present the mechanism design of the stability module and the damping module. The mechanisms are discussed in separate sections as the components separately in other prosthetic designs or in a combination as shown in this article. Second, we report the experimental protocol and the validation results from the testing of a fully functional prosthetic knee prototype on a single subject with above-knee amputation in India. The two modules were integrated into the prototype for testing. Finally, we discuss the modular adaptability, clinical implications, and limitations of the two modules.

2 Stability Module: Four-Bar Latch

2.1 Stability in the Prosthetic Knee Function. The gait cycle of able-bodied, level-ground walking for each leg can be divided into the stance phase and the swing phase (Fig. 1(*a*)). During stance, the foot is in contact with the ground. The corresponding interaction force between the foot and the ground is the ground reaction force (GRF), and the point of application of the GRF is the center of pressure (COP). The knee flexion angle is less than 20 deg during early-stance to mid-stance. During the transition from stance to swing, the foot takes off from the ground and reaches a peak knee flexion of about 64 deg during mid-swing (Fig. 1(*a*)) [12,20].

As the COP progresses from the heel toward the toe during able-bodied walking, the GRF vector exerts an external flexion moment at the knee during early stance, an external extension moment during mid-stance, and an external flexion moment during late stance (Fig. 1(*b*)) [21]. In an able-bodied person, the large flexion moment exerted by the GRF at the knee during early stance is stabilized by the physiological knee musculature exerting an opposite extension moment, which peaks at a mean of 0.7 Nm/kg (normalized to body mass) [22]. In an above-knee prosthesis user, if the prosthetic knee joint does not provide this counter moment, it can collapse due to uncontrolled knee flexion and cause the user to fall during early stance (referred to as "buckling" of the knee joint). During mid-stance, the prosthetic knee is safe against buckling, as the direction of moment changes to extension. During late stance, the moment changes again to a flexion moment due to the anterior position of the physiological hip with respect to the foot, which helps the knee flex up to 30–35 deg before transitioning into swing (Fig. 1(*a*)). During early stance, the most critical function of a prosthetic knee joint is to provide stability and prevent buckling. During late stance, controlled instability is required to achieve flexion in the prosthetic knee (equivalent to a damped joint), which helps the leg transition to swing phase. An ideal prosthetic knee would provide both of these functions, which are in conflict with each other due to the opposite nature of the desired mechanical response. However, both functions are crucial to achieving the closest possible replication of able-bodied knee kinematics in lower limb prosthesis users (Fig. 1(*a*)). Active prosthetic knees achieve this dual function efficiently by using electromechanical actuators and sensors, which can be controlled precisely by a programmable microprocessor [20]. However, achieving the same in passive prosthetics is challenging and often requires a compact implementation of complex mechanisms [20,23,24].

Different mechanisms have been designed to achieve this trade-off between stability during early stance and controlled flexion during late stance. Most of the affordable, passive prosthetic knee mechanisms designed for the developing world prioritize stability over achieving timely and optimal late stance flexion [8,20,25]. This prioritization is driven by the need to prevent accidental falls due to buckling [24]. The prevention of buckling in the passive knee mechanisms designed for the developing world can be analyzed using flexion zone diagrams (Fig. 2) [21,24].

The Jaipur exoskeleton knee (Fig. 2(*a*)) is a single-axis knee with a large flexion zone, which necessitates the use of a mechanical lock at all times to prevent the knee from buckling.[2] This hyperstability against buckling prevents any flexion at the knee during stance or swing. A user of this device is often forced to employ an undesirable "peg-leg" gait, which involves circumduction and vaulting of the prosthetic limb to achieve ground clearance during swing.

Polycentric knees, such as the Jaipur four-bar knee (Fig. 2(*b*)), use a four-bar linkage to create a virtual knee axis (KA), which is posterior to the anatomical knee axis [6,24]. This virtual posterior shift of the knee axis prevents buckling during early stance, as the GRF vector causes a stable extension moment about the virtual knee axis, keeping the knee locked at full extension (equivalent to 0 deg of flexion). The resulting flexion zone is smaller in area compared to the exoskeleton knee, which makes the

[2] http://jaipurfoot.org/

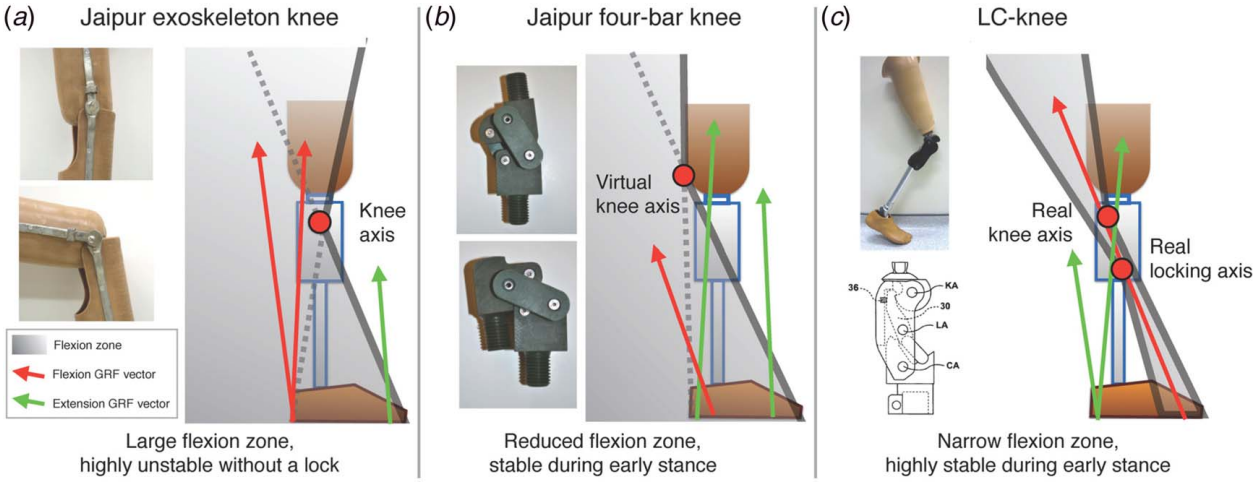

Fig. 2 Flexion zone diagrams for passive prosthetic knee mechanisms specifically designed for the developing world. Vectors in red show GRF orientations that fall within the flexion zone (shaded in gray), which can cause the knee to buckle during early stance due to the flexion moment exerted at the knee. Vectors in green show the GRF orientation outside the flexion zone that exert an extension moment, which will keep the knee stable and locked in full extension. (*a*) The exoskeleton knee will remain straight when the lock is engaged. When the lock is not engaged, the knee is unstable and is prone to flex.[3] The knee designs in (*b*) and (*c*) show two forces that result in extension moment and one in flexion [6,21,24]. LC-knee mechanism illustration adapted from US patent no. 7,087,090 [26].

polycentric design more stable against buckling during early stance. During late stance, the virtual axis is shifted continuously in the anterior direction by opening up the four-bar linkage, achieved by conscious exertion of a flexion moment from the user's hip on the prosthetic side. The anterior shift of the virtual axis also aids the flexion moment from the GRF, which enables knee flexion in late stance. Although the four-bar polycentric mechanism prevents hyperstability, it can still delay flexion and cause an untimely transition from late stance to swing, resulting in a conspicuous, asymmetric gait [8,20,24].

The LC-knee (Fig. 2(*c*)) mechanism achieves the dual functionality (of stability and flexion) efficiently in a single-axis knee architecture [21]. It provides a narrow band of flexion zone by implementing a latch mounted on a physical locking axis. This latch is biased to keep the knee locked during early stance, reinforced by the flexion moment exerted by the GRF about the locking axis. The latch unlocks during mid-stance due to the extension moment of the GRF, which frees up the knee for flexion much earlier compared to the polycentric mechanism. However, the flexion zone in the LC-knee is a very narrow band, which requires the user to actuate flexion by consciously orienting the GRF within this band using the hip. In addition, the LC-knee may also lead to hyperstability during walking on slopes and inclines due to the narrow band of the flexion zone around the knee joint.

2.2 Mechanism Design and Operation. We present a novel mechanism for the stability module, which was designed to achieve the dual function of stability during early stance and controlled instability that allows knee flexion during late stance. The mechanism of this module was implemented by a latch mounted on a four-bar linkage with a low and distal (close to the foot) (virtual locking axis (VLA)), the instantaneous center of rotation of the four-bar linkage, which widens the flexion zone near the knee but keeps it narrow near the foot.

The main components of the mechanism include (Fig. 3(*a*)): (i) the knee piece, which is connected proximally to the socket and rotates about the KA, (ii) the links of the four-bar mechanism that are mounted on the body frame of the mechanism and create a VLA for the latch, and (iii) the latch, which serves as the coupler link for the four-bar linkage. The latch is connected distally to the pylon and proximally to the body shell of the mechanism (through the four-bar linkage). In addition, there is a hard stop that limits the rotation of the knee piece and the latch beyond 0 deg, preventing any hyperextension of the knee (counterclockwise direction in Fig. 3(*f*)). The stepwise operation of the stability module at key points during the gait cycle is described with a cross-sectional view of the mechanism in the sagittal plane (Figs. 3(*b*)–3(*e*)).

The latching mechanism involves four major steps, the first two occurring during stance (Figs. 3(*b*) and 3(*c*)) and the latter two occurring during swing (Figs. 3(*d*) and 3(*e*)):

(1) Locked position (Fig. 3(*b*)): As the user's heel-region strikes the ground during early stance, the mechanism experiences a GRF flexion moment about the knee axis. The latch is in a pre-locked position due to the pre-loaded bias spring. Buckling is prevented by the mechanical engagement of the proximal knee piece with the latch tip. The locking action is also reinforced by the flexion moment about the virtual axis of the four-bar linkage, which ensures that the latch remains engaged against the knee piece during early stance.
(2) Latch unlocking (Fig. 3(*c*)): During mid-stance, the user rolls over on the foot and the GRF vector moves anterior to the knee axis and the virtual axis. The distal portion of the knee joint can translate back on the four-bar linkage, which unlatches the stability module. The proximal knee piece experiences an extension moment about the knee axis, which disengages it from the latch tip. The latch also experiences an extension moment about the virtual axis, allowing it to move freely backward (via the four-bar linkage), compressing the bias spring. With the latch in the unlocked position, the knee is freed to initiate flexion. The knee flexes under a GRF flexion moment during late stance, as the GRF vector passes through the flexion zone, which is the area posterior to the knee axis and anterior to the VLA.
(3) Latch repositioning (Fig. 3(*d*)): Once the knee has flexed through late stance and swing has been initiated, there is no GRF-induced moment on the four-bar linkage. The location of the lower leg is controlled using the swing module (in case of this design using the damping module described in Sec. 3). The restoring force from the bias spring returns the

[3]See Note 2.

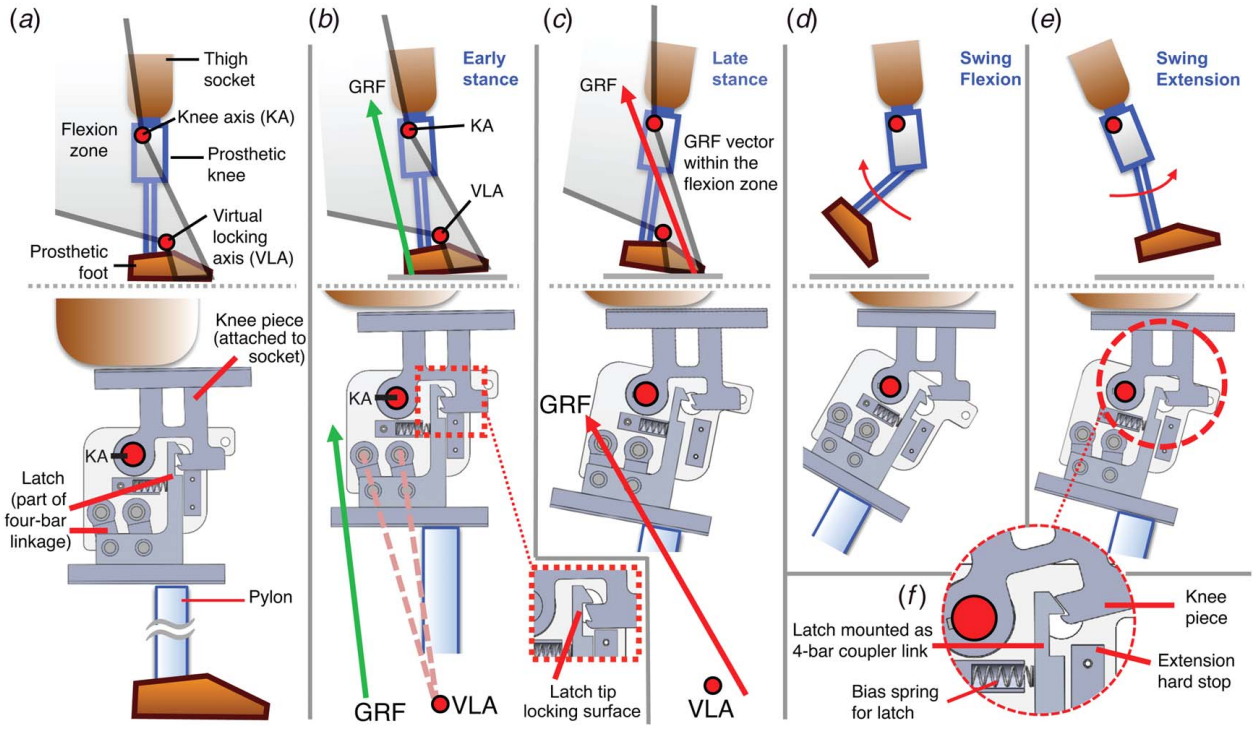

Fig. 3 Operation of the stability module mechanism through the gait cycle (*a–f*). (*a*) Cross-sectional view of the mechanism with the major parts labeled. (*b*) Early stance: the latch is engaged; therefore, the knee is locked and the GRF vector reinforces the latching action between the latch tip and the knee piece by applying a flexion moment about the virtual locking axis (VLA). (*c*) Late stance: the latch is disengaged (the unlatching is exaggerated for clarity), and flexion is initiated, because the GRF vector (red arrow) is oriented in the flexion zone between the knee axis and VLA. (*d*) Swing phase flexion: the latch is ready to be engaged. (*e*) Swing phase extension: the latch engages with the knee piece at the end of swing. (*f*) The inset shows a close-up of the latch tip interaction with the knee piece during locking at the end of swing. This double-latch feature allows the mechanism to lock at an intermediate point for safety against buckling.

latch to the forward position, ready to lock again at the end of swing.

(4) Latch relocking (Fig. 3(*e*)): As the lower leg and foot swing forward to extend the knee at the end of the gait cycle, the knee comes down on the latch tip, pushing it back against the spring until the knee has extended far enough to allow the restoring spring force to relock the knee. In the relocking step (Fig. 3(*f*)), there is a unique feature in the knee piece that allows for relocking at two different points, referred to as a double latch. This feature allows the mechanism to lock at an intermediate point before reaching full extension (designed to be at 10 deg of knee flexion). This feature prevents accidental buckling as it ensures that the knee will lock even if the user does not fully extend the knee before heel strike of the next gait cycle, as may happen while walking up inclines.

A fully functioning prototype of the stability module mechanism was built using machined parts. The material for the latch was selected by calculating the safety factor using finite element analysis of the latch under maximum flexion moment from the GRF. Aluminum 7075 alloy was used to achieve a safety factor of 1.2 (von Mises yield stress) in the latch for the maximum flexion moment during stance exerted by a hypothetical user with 100 kg body mass. Aluminum 6061 alloy was used for the rest of the parts in the assembly. To prevent fatigue-induced failure, the prototype was not subjected to more than a few hundred cycles of loading during human subject testing. Therefore, fatigue analysis was not performed to account for the failure modes due to the cyclic loading of the mechanism.

2.2.1 Placement of the Virtual Locking Axis. In a normal gait cycle, the COP progresses along the plantar surface of the foot from the heel to the toe during stance (Fig. 4). The COP location and the corresponding orientation of the GRF vector in space were deterministically used to unlock the latch at the desired instant in the gait cycle, called the GRF transition point. To replicate the able-bodied knee kinematics through stance, the GRF transition point was chosen at the COP that corresponds to the initiation of late stance flexion in an able-bodied knee (Fig. 4) [22]. As the COP passes through this selected GRF transition point, it was desired

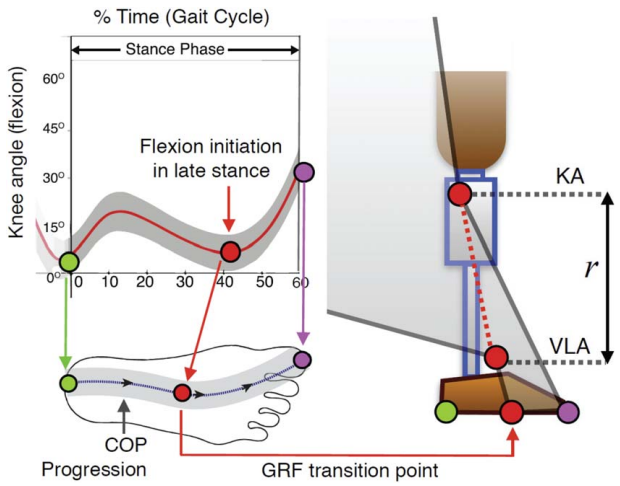

Fig. 4 Starting point for placement of the VLA. The GRF transition point is the point at which the latch is disengaged, which was chosen to coincide with the COP instance that corresponds to initiation of knee flexion in able-bodied walking.

that the latch would go from being locked to unlocked, which would allow the knee to flex into swing.

To ensure this timely unlocking of the latch at the "GRF transition point," the starting point for setting the VLA position was constrained to the line connecting the GRF transition point and the knee axis (shown by a dashed line in Fig. 4). Placing the VLA in this position ensures that there exists a point along the dashed line where a GRF vector anterior to the line exerts a flexion moment at the knee; any GRF vector that is anterior to the GRF transition point and passes between VLA and the KA will cause the latch to disengage and apply a flexion moment about the KA, causing the knee to flex. After, 1 based on the additional goal of minimizing hyperextension.

As the latch unlocks during mid-stance extension, the hyperextension results in a small posterior motion of the lower leg. This movement may be perceived by users as an uncomfortable, backward wobble at the prosthetic knee [15]. Based on pilot studies with an earlier prototype design that used a physical locking axis within the knee, users reported the ability to distinctly feel the angular motion between the upper and lower leg of up to 3 deg hyperextension, which led to discomfort and reduced confidence in the performance of the prosthesis [15]. In the present mechanism, we minimized hyperextension to only 1 deg at the VLA; given the distal position of the VLA to the KA, this small angular deflection translates the latch posterior with respect to the knee piece using the four-bar linkage, causing the stability module to unlatch. With the latch movement set at 5 mm (chosen to ensure required strength and secure unlocking), the four-bar linkage sets the resulting virtual locking axis location 30 cm distal to the knee axis for a hypothetical user [22]. A low, distal locking axis was therefore implemented to reduce hyperextension through the use of a four-bar latch mechanism. In addition, this maximized the area of flexion zone at the knee while keeping it narrow near the foot (Fig. 4). This flexion zone can allow a wide orientation of GRF vectors in the toe region to flex the knee during late stance without compromising stability during early stance.

The process outlined earlier is a general process for setting the placement of the VLA. Adjustments to the mechanism geometry may be required depending on whether the prosthetic foot GRFs and CoP vary significantly from able-bodied values. Additional fine-tuning might be desired based on other subject-specific requirements and alignment suggestions from the prosthetist. The final dimensions of the four-bar linkage presented in this article are included in the Appendix.

2.3 Potential Advantages Over Prior Art. The stability module mechanism offers potential functional advantages over prior art:

(1) The locking axis could be implemented either through a physical axis or through a virtual axis using a four-bar linkage. The physical axis uses fewer parts but requires a longer body shell to place the locking axis sufficiently away in the distal direction (implemented in the LC-knee [21]). The choice of a virtual axis implementation using a four-bar linkage allows flexibility in placing the locking axis distally further with a more compact mechanism compared to the LC-knee.
(2) The mechanism provides an optimal flexion zone by widening the flexion zone near the knee while maintaining a narrow flexion zone near the foot. This layout of the flexion zone allows for easy flexion during late stance without compromising stability during early stance. This was made possible due to the low, distal location of the virtual locking axis enabled by the four-bar linkage. In addition, this distal location also minimized the hyperextension angle at the knee.
(3) We used a geometric method to compute the location of the virtual locking axis, which informed its precise location. In the clinical context, this knowledge of the exact location of the locking axis in space can help the prosthetist easily align the prosthetic knee with respect to the prosthetic foot. The relative position of the foot and the knee could be manipulated systematically by the prosthetist to further widen or narrow the flexion zone available to a particular user.

3 Damping Module: Rotary Viscous Damper

3.1 Damping in the Prosthetic Knee Function. Damping in prosthetic knees is primarily required to decelerate the flexion of the knee during the transition from stance to swing [20]. This transition starts in late stance and ends in mid-swing with a mean peak knee flexion of around 64 deg (Figs. 5(*a*) and 1(*a*)) [12]. In the absence of sufficient damping during knee flexion, the prosthetic knee can overshoot well beyond the peak flexion of the knee required for ground clearance, delaying the swing phase for the prosthetic leg. Conversely, if the damping torque is greater than the optimal value, the knee does not flex enough, which can force the user to employ alternative strategies to achieve safe toe clearance in swing such as hip-hiking, vaulting, and circumduction [27]. Such asymmetric gait patterns between the able-bodied leg and the amputated leg are undesirable, as they can increase metabolic energy expenditure [27]. In addition, in the context of developing countries such as India, the focus on achieving close to able-bodied gait behavior has been shown to be one of the most important design requirements for prosthesis users [4]. Therefore, achieving peak knee flexion during swing that is within the able-bodied range (64 ± 6 deg) is crucial for the performance of passive knee prostheses [12].

A wide array of prosthetic knees have been designed to provide damping control of knee flexion in late stance and swing. Primarily designed for persons with amputation in developed countries, popular knee prostheses have incorporated fluid-based (pneumatic or hydraulic) systems, which can be controlled passively, or through programmable, microprocessor-controlled actuators that deliver high kinematic performance by implementing sensor-based feedback control [20,28]. Affordable prosthetic knee joints designed primarily for the developing world have incorporated passive friction brakes that provide fixed resistance during flexion [28]. Though implementation of friction brakes is simple and cost effective, it also presents many practical challenges such as torque changes due to wear and changing environmental conditions, such as humidity or rain [16]. Moreover, friction brakes provide constant resistance, which makes them unresponsive to changes in the walking speed as the damping torque required in a prosthetic knee changes appreciably with walking speed [20,29,30].

In prosthetic knee technology, the most common passive architecture of fluid-based dampers is the hydraulic cylinder. It commonly incorporates a piston to push a viscous oil between two chambers through a small orifice with adjustable diameter [31,32]. This architecture borrows from the prevalent design of hydraulic cylinders used in other industries (automotive vehicles, construction technology, consumer goods, etc.) [33]. Hydraulic dampers have been preferred over friction brakes as they offer smooth, speed-based resistance. However, hydraulic cylinders in prostheses are expensive, heavy, and require periodic maintenance to prevent oil-leaks [28]. Mechanical integration of hydraulic cylinders about a rotating knee joint requires an additional linkage, which can make the prosthesis assembly bulky and heavy. The resistive force offered by hydraulic cylinders is proportional to the square of piston velocity (piston velocity changes linearly with walking speed). This nonlinear relationship is relevant for a small fraction of prosthesis users who can vary their walking speeds over a large range (1–1.8 m/s) using active, microprocessor-controlled knees [20]. At faster walking speeds, the knee moment increases in proportion to the square of the walking speed (or knee angular velocity, which scales in proportion to the walking speed) [12,29]. However, at slower walking speeds, the knee moment changes linearly with small changes in speed. Most users of passive prostheses indeed walk slower (0.8–1.2 m/s) and

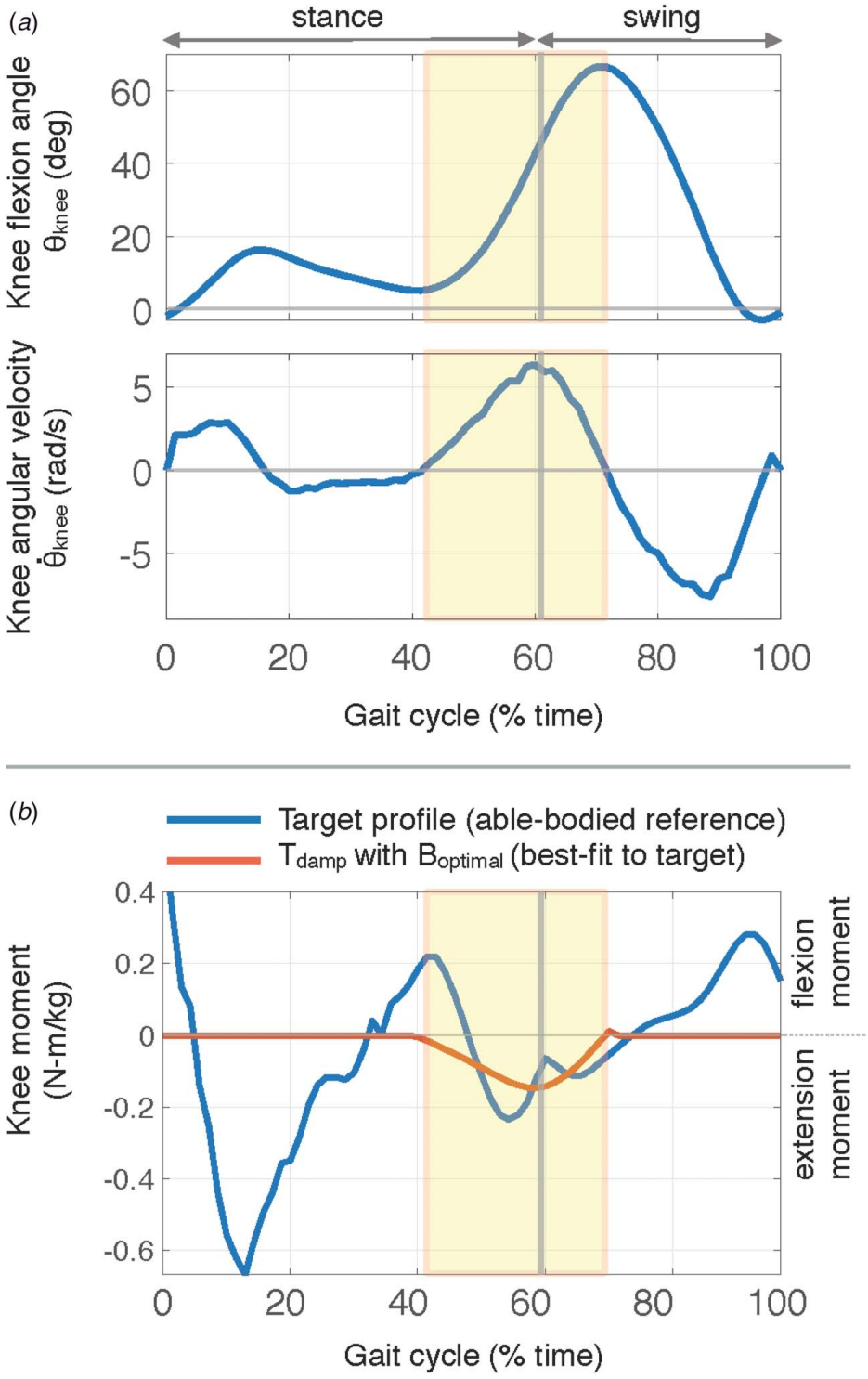

Fig. 5 Target damping coefficient computation. (*a*) Mean knee flexion kinematics (angle and angular velocity) for an able-bodied person [22]. The damping zone of interest is highlighted (shaded region). (*b*) Target knee moment was used to estimate the optimal damping torque in the damping zone (T_{damp} in Eq. (1)).

require resistance that is linearly proportional to small changes to their preferred walking speed [20,29,31,32].

To address the aforementioned limitations of traditional hydraulic dampers, we present the design and preliminary validation of a rotary viscous damper that is compatible with low-cost, single-axis prosthetic knees. This damper provides torque that is linearly dependent on the walking speed by implementing a shear-driven, first-order resistance to fluid flow. In addition, the rotary architecture enables easy assembly of the damper in the existing architecture of low-cost, single-axis prosthetic knee units.

3.2 Target Damping Coefficient. In a mechanical system, the magnitude of the damping coefficient characterizes the resistance offered by a damper. In the design of a damper, the primary functional specification that needs to be achieved is the damping

coefficient. The fundamental objective of our damping module was to achieve the appropriate resistance required to enable close replication of able-bodied kinematics during late stance and swing for level-ground walking and only body-weight loading, as the kinematics and kinetics change in other cases. Therefore, as a first step toward designing an optimal damping module, the range of target damping coefficients required for best possible replication of able-bodied kinematics during knee flexion was determined from published literature (for a fully passive damper). Publicly available reference gait data from 19 able-bodied persons [34] and the computational methods presented by Narang et al. [13,14] were used to determine the target damping coefficient. Only a brief summary is presented here.

Mean knee kinetics (moment) and mean knee kinematics (flexion angle and angular velocity) data from able-bodied subjects walking at self-selected speed on level-ground were used as reference targets [34]. A typical example of the mean knee kinematics profile (knee angle and angular velocity) for an able-bodied person is shown in Fig. 5(*a*) [22]. A rotary viscous damper was modeled to engage in the knee during the transition from stance to swing. The damping module is applied starting in late stance, right as the stability module unlatches, and is engaged until the knee maximum flexion during swing. The corresponding section of the knee flexion curve is highlighted in Fig. 5(*a*) (0–64 deg in case of full leg extension during mid-stance), hereby referred to as the "damping zone" of the gait cycle. The rotary hydraulic damper acting at the knee was modeled as an ideal, first-order, shear-based viscous damping element, formulated mathematically as follows:

$$T_{damp} = -B \cdot \dot{\theta}_{knee} \tag{1}$$

where T_{damp} is the damping torque (Nm), expressed as the product of the reference knee angular velocity over the damping zone, $\dot{\theta}_{knee}$ (rad/s), and B, the damping coefficient (Nm/rad/s).

To estimate the optimal damping coefficient, the damping torque T_{damp} profiles were computed for a range of damping coefficients (0–5 Nm/rad/s) using Eq. (1). Over the damping zone, each T_{damp} profile was compared with the target knee moment profile (Fig. 5(*b*)). The damping torque profile with the highest coefficient of determination (R^2) was selected. The corresponding damping coefficient was identified as the optimal damping coefficient, $B_{optimal}$ (Fig. 5(*b*)). The value of $B_{optimal}$ was found to be 1.5×10^{-2} Nm/rad/s/kg (normalized to the body mass). Based on the exact body mass of a prospective user, a damper prototype with appropriately scaled $B_{optimal}$ was hypothesized to enable close replication of able-bodied kinematics during knee flexion. For a person with body mass of 75 kg, the value of target $B_{optimal}$ is 1.13 Nm/rad/s.

For persons with body mass ranging between 50 and 100 kg, the range of nonnormalized $B_{optimal}$ is 0.75–1.50 Nm/rad/s. This range of $B_{optimal}$ served as the target range of damping coefficients to be achieved through the mechanism design of the damping module to achieve peak knee flexion during swing that is within the able-bodied range (64 ± 6 deg for users with body mass in the range of 50–100 kg).

3.3 Mechanism Design and Operation. The damping module was constructed to generate a high damping torque by shearing a thin film of high-viscosity silicone oil. The principle of shearing a thin film of fluid to generate a high braking force has been used widely across many industries in different mechanical embodiments. Common examples include automotive viscous couplings, engine vibration dampers, tripod joints, and press brakes [34,35].[4] In active knees, the magnetorheological fluid damper has been implemented in the shear-mode for low-speed walking [29,36,37]. However, to our knowledge, shear-based damping has not been explored in passive prosthetic knees due to the widespread adoption of traditional cylindrical and rotary hydraulic dampers.

The detailed construction of our rotary damper prototype is illustrated in Fig. 6. The damping torque is generated by shearing a highly viscous fluid trapped between the stator and rotor plates, which are annulus-shaped plates that are coaxially stacked about the knee axis. The stator plates are coupled to the cylindrical housing by four projecting tabs on the outer edge, which mesh into the keyways on the inner circumferential wall of the housing (Fig. 6(*a*)). The rotor plates are coupled to the rotating shaft of the prosthetic knee by four projecting tabs on the inner edge, which mesh into the keyways on the rotor clutch. This coupling

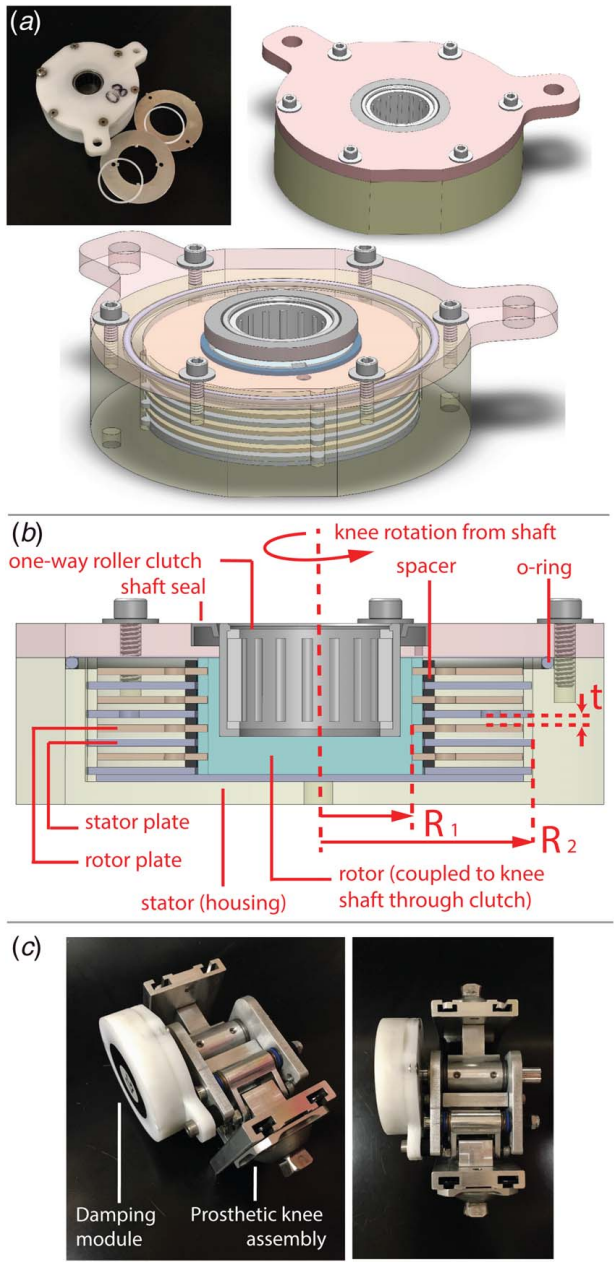

Fig. 6 Design of the damping module. (*a*) Prototype: photograph and computer-aided design (CAD) of the final assembly. A stator plate, a rotor plate, and spacers are shown in the photograph. (*b*) Cross-sectional view of the prototype. Silicone oil is trapped between the rotor and stator plates to provide resistive shear torque. (*c*) The damping module was mounted co-axial to the prosthetic knee axis, as shown. The damper housing was bolted to the shell of the prosthetic knee to provide rotational constraint.

[4] http://www.clearcoproducts.com/

ensures that the rotor plates turn with the prosthetic knee shaft, as the knee rotates in flexion. The housing is static relative to the rotating shaft, as it is rigidly coupled to the prosthetic knee assembly (Fig. 6(*c*)). Spacers of specific height are placed between the consecutive stator and rotor plates. The small gap between the neighboring plates is fully filled with the viscous liquid (Fig. 6(*b*)). As the knee flexes, the rotor plates rotate with respect to the stator plates, shearing the viscous fluid in between the plates. The resulting damping torque between the neighboring stator–rotor plate combination is quantified by the following relationship, derived by integrating the viscous shear stress caused by Couette flow of the liquid along the annular area of the plates [38]:

$$B_{plate} = \frac{T_{damp}}{\dot{\theta}_{knee}} = \frac{\pi\mu}{2t}(R_2^4 - R_1^4) \tag{2}$$

where B_{plate} is the resultant damping coefficient, T_{damp} is the viscous damping torque, $\dot{\theta}_{knee}$ is the angular velocity of the knee joint, μ is the dynamic viscosity of the fluid, t is the thickness of the gap between the stator plate and rotor plate, R_2 is the outer radius of the stator or rotor plate annulus, and R_1 is the inner radius of the stator or rotor plate annulus. These variables are annotated in Fig. 6(*b*).

The total damping torque for multiple neighboring stator–rotor plates, as illustrated in Fig. 6, is expressed as follows:

$$B_{total} = (2n) \cdot B_{plate} \tag{3}$$

where n is the number of rotor plates stacked between two neighboring stator surfaces; $n = 4$ in Fig. 6(*b*).

The housing and the housing cap of the damper prototype were machined out of Polyacetal (Delrin). The stator and rotor plates were made using Aluminum 6061 alloy sheets (Fig. 6(*a*)). The spacers placed between the stator and rotor plates were made out of precision shim stock of Polyacetal (±25 μm tolerance). The rotor plates were coupled to a one-way roller clutch, which in turn was coupled to the rotating knee shaft (Fig. 6(*b*)). The one-way roller clutch ensured that damping was enabled only within the damping zone, i.e., during the knee flexion of late stance and swing (Fig. 5(*a*)). During knee extension, there was no-damping torque generated and the knee shaft rotated freely within the roller clutch.

The viscous fluid used in the damper consisted of polydimethylsiloxane, a silicone oil with a very high kinematic viscosity of 100,000 centistokes (Clearco Products, Willow Grove, PA). The dynamic viscosity of the oil is 100 Pa s; for comparison, the dynamic viscosity of water is 1 mPa s. The oil displays a characteristic shear-thinning behavior, with an apparent reduction in viscosity as the shear rate or velocity gradient increases [38]. To account for this dynamic change in viscosity, the damping torque calculation was adjusted based on the shear-thinning data provided by the manufacturer.[5] Below the critical velocity gradient (30 s^{-1}), the fluid behaves like a Newtonian fluid with a near constant kinematic viscosity of 100,000 centistokes. At velocity gradients higher than 30 s^{-1}, the kinematic viscosity drops in accordance to the following empirical power law relationship reported by the manufacturer[6]:

$$\mu_{kin} = (4.32 \times 10^5) \cdot (v_{grad})^{-0.43} \tag{4}$$

where μ_{kin} is the kinematic viscosity of the fluid in centistokes and v_{grad} is the magnitude of the velocity gradient or shear rate for a fluid flowing between two parallel plates (in s^{-1}), which is computed as the ratio of the speed of the moving plate and the distance between the moving and stationary plates.

The prototype was assembled in multiple stages. Starting from the bottom surface of the housing, a stator–rotor plate pair was stacked between the housing and the rotor (concentric to the knee axis). A small, incremental volume of viscous oil was then injected into the housing sufficient to fill up the space between the plate. The oil was injected from the top. The prototype was then placed in a vacuum chamber to minimize the entrapment of air bubbles in the oil. Two small, diametrically opposite holes were also incorporated in the plates to facilitate complete filling of the space between the plates. This process was repeated in vacuum for each addition of a stator–rotor plate pair in the stack. After all the plates were installed with oil between them, the fully assembled stack was sealed off with an o-ring between the housing and the cap, which was bolted on top of the housing. A rotary shaft seal was incorporated between the rotating assembly and the stationary housing (Fig. 6(*b*)).

Two prototypes of the damping module were built with five and six pairs of rotor–stator plates, respectively ($n = 5$ and $n = 6$, $R_2 = 30$ mm, $R_1 = 17.5$ mm, $t = 0.8$ mm, and $\mu = 100$ Pa s). The resulting damping module prototypes weighed approximately 0.2 kg; the fully assembled prosthetic knee prototype weighed approximately 1.3 kg. The mean damping coefficients for the two prototypes were designed to be 1.11 Nm/rad/s and 1.33 Nm/rad/s, respectively, as calculated using Eqs. (2) and (3). The five-plate damper prototype was ideal for a 75 kg user, and the six-plate damper prototype was ideal for an 88 kg user. These damping coefficients were within the target range of optimal damping coefficients (0.75–1.49 Nm/rad/s) based on the range of body masses of most users (50–100 kg), as laid out in Sec. 3.2.

3.4 Damper Characterization. The theoretical model for the design of the damper prototypes (Eqs. (2) and (3)) was investigated by a damper tester built specifically for the empirical characterization of the torque-velocity relationship of the two damper prototypes (Fig. 7(*a*)). A velocity-controlled DC motor (VexRobotics, Greenville, TX) was used to apply a constant velocity profile to the damper and a magnetic encoder was used to record and control the angular velocity. A load cell (LC101-250, Omega, Norwalk, CT) measured the force experienced by the damper at a fixed lever length. The velocity control and the data collection were performed on a Visual Basic platform supported by VexRobotics. This tester was first validated with two commercially available viscous dampers (FDT-57 and FDT-63, ACE controls, Farmington Hills, MI).[7] The experimentally measured torque–velocity relationship matched the values provided by the manufacturer of the commercial dampers within an error margin of 0.5 Nm, equivalent to 5% of the nominal damping coefficient reported by the manufacturer.

The two damper prototypes ($n = 5$ and $n = 6$) were characterized on the tester. To map the torque–velocity relationship, the motor was used to apply five different constant angular velocity profiles. These five values were chosen at equal intervals between 0 rad/s and 6 rad/s. This range was chosen based on the range of knee angular velocities observed in the gait of able-bodied people [22] (Fig. 5(*a*)). At each value of the chosen constant velocity, a total of ten rotations were completed and the damping torque was recorded continuously through the load cell. The mean damping torque was computed for each of these five values of angular velocities, along with the corresponding standard deviation.

The results from the torque–velocity characterization of the two prototypes showed that the experimentally measured damping coefficients followed the model prediction well, with R^2 values of 0.96 (five-plate damper) and 0.87 (six-plate damper) (Fig. 6(*b*)). The mean damping coefficients of the two prototypes across the velocity range were within 2% of the modeled mean values. Overall, the data matched the model well (within 10%) at higher angular velocities and showed a higher difference at lower speeds (within 30%). The difference between the measured coefficients and the modeled values could be attributed to a combination of factors such as changes in the gap between the stator and rotor plates due

[5]See Note 3.
[6]See Note 3.
[7]http://www.acecontrols.com/

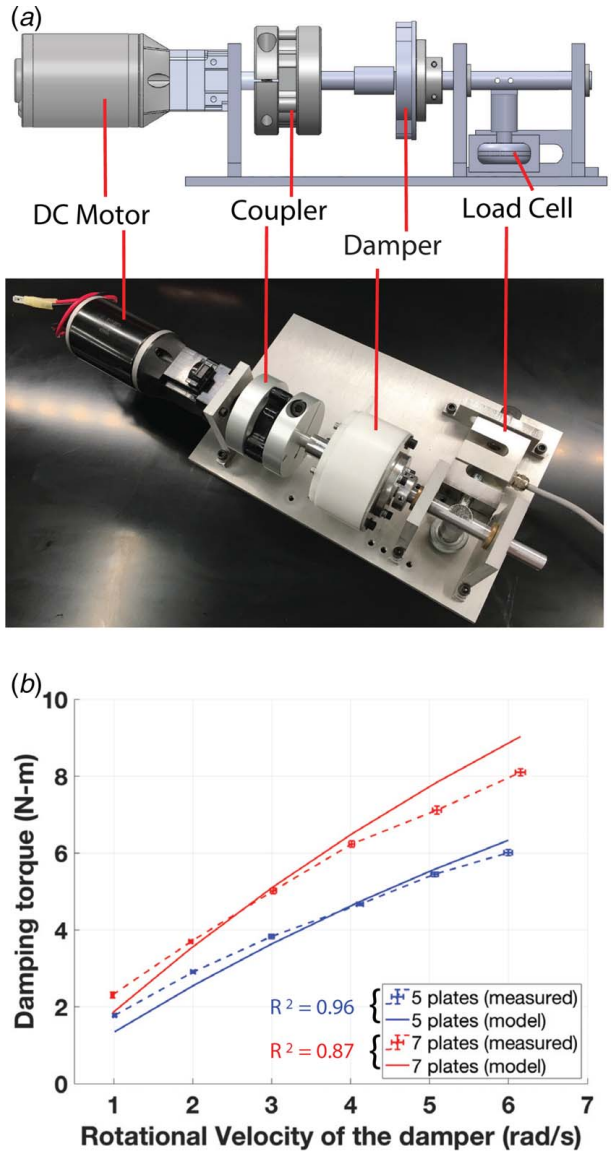

Fig. 7 Damper characterization. (*a*) Damper tester used for torque–velocity characterization of the damper prototype. The housing of the damper prototype is connected to a load cell through a lever arm to measure the torque, and the shaft is driven by the velocity-controlled DC motor. (*b*) The measured damping torque for 0–6 rad/s from the tester matched the model-based prediction closely.

to tolerance stack-up or wear, changes in viscosity due to heat generation, and uncertainty in the viscosity value of the oil. The viscosity of the oil was only accurate to within ±10% of the nominal value, as specified by the manufacturer.[8] Overall, the theoretical model was found to be a useful design tool for sizing the damper prototypes accurately for their applications in prosthetics.

4 Preliminary Testing on an Above-Knee Prosthesis User

A prototype prosthetic knee was assembled by integrating the stability module and the damping module (Fig. 8(*b*)). The primary goal of the preliminary experimental trial was to investigate the basic functionality and safety of the prototype in the real-life scenario

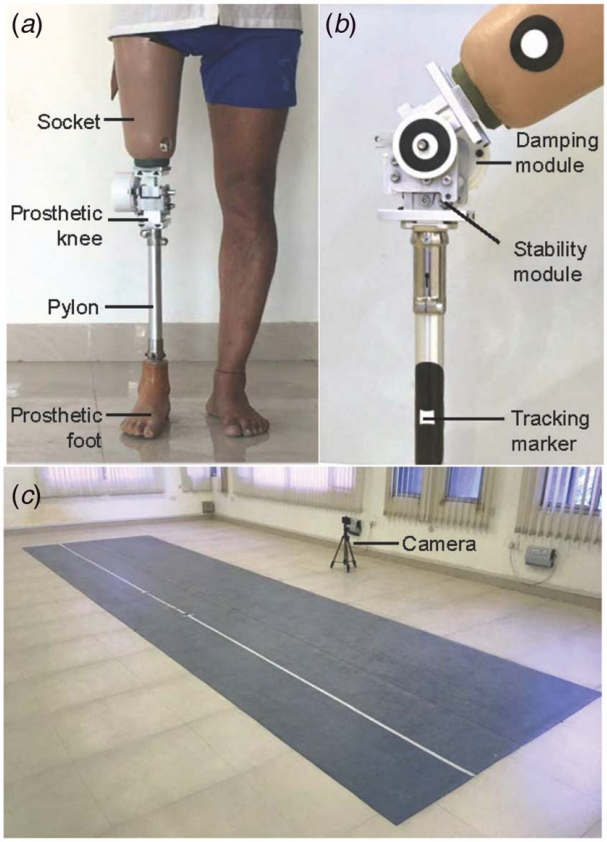

Fig. 8 Preliminary testing on a single subject with above-knee amputation in India. (*a*) The prosthetic leg assembly. (*b*) The damping module was mounted and assembled co-axial to the knee axis of the stability module. (c) The indoor walking track used for walking trials. Each trial was recorded using an iPhone camera at 240 frames per second.

of level-ground walking with the full magnitude of the GRF exerted on the knee mechanism by a person with above-knee amputation (Fig. 8).

4.1 Experimental Protocol. The experimental trial was conducted at the Jaipur Foot clinic in Jaipur, India.[9] The MIT Committee on the Use of Humans as Experimental Subjects and the Jaipur Foot clinic approved the experimental protocol. One male with above-knee limb loss was recruited as the subject for the study (body mass 75 kg and body mass index 25.8; Fig. 8). The subject had over three years of walking experience with a polycentric prosthetic knee and a single-axis exoskeleton knee (Figs. 2(*a*) and 2(*b*)), in combination with a single-part passive prosthetic foot made by the Jaipur Foot clinic. Three different damping conditions (no damping, five-plate damper, and six-plate damper) were tested in three separate walking trials. A stepwise summary of the protocol is presented here:

(1) Fitment: The prosthetic leg was assembled with the prototype prosthetic knee and the single-part prosthetic foot made by the Jaipur Foot clinic (Figs. 8(*a*) and 8(*b*)). The pylon length was adjusted based on the subject's height and the customary socket used by the subject was used for fitment. The on-site prosthetist at the clinic conducted the fitting and static alignment.
(2) Training: After the fitment, the subject was trained to walk with the prosthetic leg for 10 min with the support of parallel

[8]See Note 3.

[9]See Note 2.

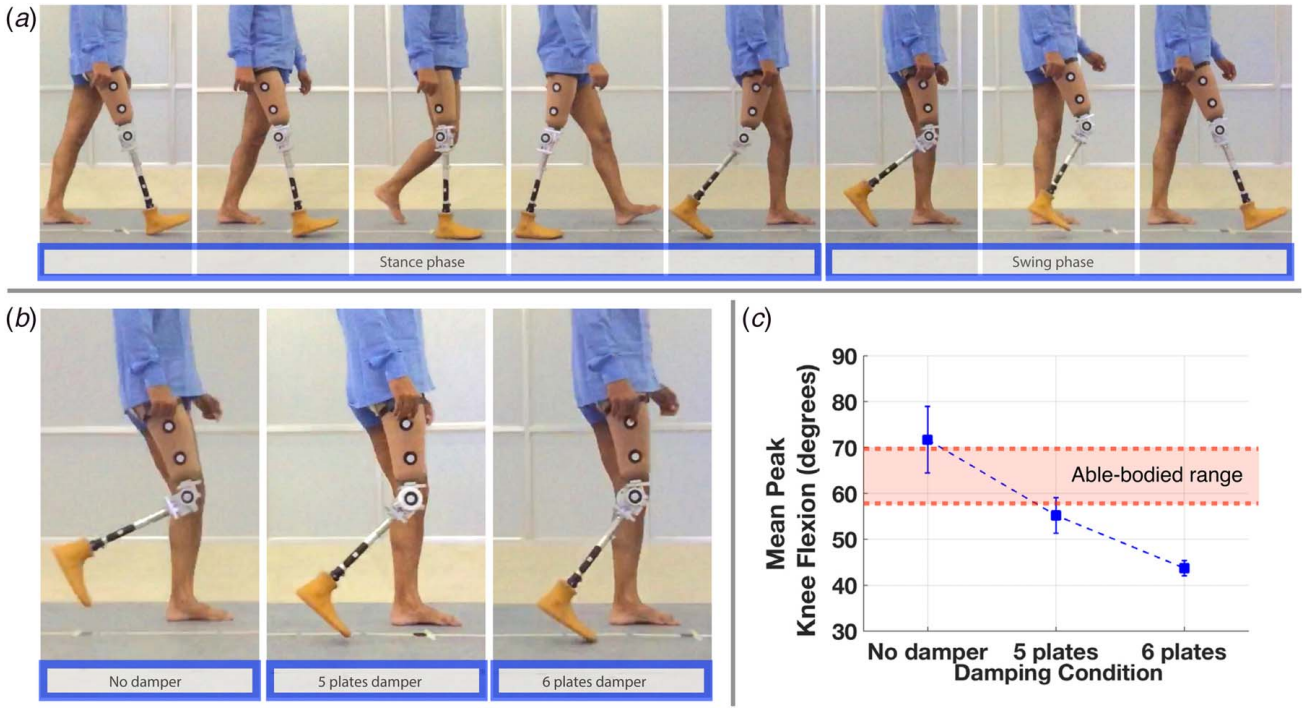

Fig. 9 Experimental trial. (*a*) Subject walked comfortably on level-ground; snapshots through a full gait cycle are shown for the first walking trial (read left to right). (*b*) Snapshots of the peak knee flexion angle in the swing phase for the three walking trials. (c) The mean peak knee flexion angle decreased with the increase in the damping coefficient. The damping coefficient could be tuned to achieve able-bodied range of peak knee flexion (shown in the shaded band).

bars. The goal of this exercise was to train the subject to use the stability module correctly by trying to initiate timely knee flexion and transition safely from stance to swing. After the subject felt confident, the safety rails were removed and the subject walked freely on level-ground without any support for about 10–15 min at a relaxed cadence. The prosthetist observed for any conspicuous gait deviations that could be corrected through dynamic alignment of the prosthetic knee and foot.

(3) Trials: Three indoor walking trials were conducted with each trial involving level-ground walking for at least 5 min. The subject was asked to walk back and forth on a straight walkway of 15 m length (Fig. 8(*c*)). In each trial, the stability module remained the same, and three different damping conditions were tested sequentially: no damping, five-plate damper (ideal), and six-plate damper (high), respectively. The subject was asked to walk at a comfortable, self-selected speed during each trial. The subject was blinded to the order of damping conditions.

(4) Data collection: Video of each walking trial was recorded using an iPhone camera at 240 frames per second (Apple Inc, Cupertino, CA). The camera was mounted on a tripod, parallel to the walkway (Fig. 8(*c*)). Flat white circular markers with a black background were placed on the lateral side of the socket, knee joint, and the pylon (Fig. 8(*b*)). To determine the knee angle in the sagittal plane, the kinematics of the markers were tracked in the video using an open-source motion tracking software (DLTdv, Chapel Hill, NC) [39]. The upper leg (residual limb and socket) and the lower prosthetic leg were assumed to behave as rigid bodies. The knee angle in the sagittal plane was computed as the difference between the upper leg and the lower leg orientation in the sagittal plane (Fig. 1(*a*)). Data smoothing was performed using a low-pass Butterworth filter. The peak knee angle during each recorded step that was captured by the camera was computed and averaged over the trial. At least five steps were recorded during each walking trial.

(5) Feedback: Each trial was monitored by the on-site prosthetist for safety. At the end of each trial, the subject was interviewed with open-ended interview questions designed to elicit qualitative feedback. After the completion of the three trials, the stability module and the two dampers were visually inspected for any signs of wear, mechanical failure, and oil leakage.

5 Results

5.1 Stability Module. The subject was able to use the latch mechanism efficiently during the training period. The stability module functioned as expected, enabling smooth stance to swing transition while allowing the knee to flex during late stance (Fig. 9(*a*)). If the prototype did not unlatch correctly, the subject would have retained a straight leg into late stance and swing, which would likely lead to a stumble. No stumbles were observed during the three walking trials. Inspection of the mechanism after the trials showed no signs of mechanical failure.

In the feedback interview, the subject reported "smooth and intuitive" control and appreciated the locking feature of the stability module. In comparison to the polycentric knee that the subject had been using, they reported a "greater sense of safety" during early stance. The subject expressed a strong disapproval of the loud, clicking noise of the latching mechanism and emphasized the need to have an aesthetically pleasing cosmesis to enclose the mechanism of the prototype.

5.2 Damping Module. According to the preliminary results, each of the three damping conditions had a direct effect on the peak knee flexion angle achieved by the user during the walking trials (Fig. 9(*b*)):

(1) In the first walking trial, no damper was incorporated in the prosthetic knee and the mean peak knee flexion was 71.7 ± 7.3 deg (SD).
(2) In the second walking trial, the five-plate damper prototype was used. The damper had a mean damping coefficient of 1.11 Nm/rad/s, as characterized by the damper tester. This damping coefficient value was close to the target damping coefficient required to enable peak knee flexion in the able-bodied range for the subject ($B_{optimal} = 1.13$ Nm/rad/s for 75 kg subject body mass, as discussed in Sec. 3.2). The mean peak knee flexion angle in this trial was 55.2 ± 3.9 deg, and the estimated knee angular velocity was 6.4 rad/s.
(3) In the third walking trial, the six-plate damper was used, which had a mean damping coefficient of 1.33 Nm/rad/s. This damping coefficient was higher than the target damping coefficient for the subject (1.11 Nm/rad/s). The mean peak knee flexion angle was 43.7 ± 1.6 deg, and the estimated knee angular velocity was 5.7 rad/s.

In the feedback interview, the subject reported discomfort in initiating flexion due to "heavy resistance" in the third walking trial with the six-plate damper. The subject was not able to perceive any significant difference between the no-damping condition and five-plate damper. The dampers were visually inspected after the walking trials. No conspicuous signs of mechanical failure or leakage were found.

6 Discussion

6.1 The Effect of Damping on Peak Knee Flexion. The results from the preliminary testing of dampers on a single individual with above-knee amputation showed a clear trend (Fig. 9(*c*)). An increase in the first-order damping coefficient led to a decrease in the peak knee flexion during swing. Multiple studies have reported a similar trend for traditional hydraulic dampers and friction-based dampers [21,29]. In the no-damping condition, the peak knee flexion was slightly higher than the able-bodied range. The peak knee flexion in the able-bodied population is approximately 64 ± 6 deg (1 SD) [13]. The five-plate damper achieved knee flexion closer to the able-bodied range. With the six-plate damper, the observed knee flexion was much smaller than the able-bodied target, as indicated by the computational model used to compute the target damping coefficient. These results demonstrate the importance of damping during late stance and swing phases of walking. With the appropriate magnitude of first-order damping tuned for each user, knee flexion in the able-bodied range can be achieved in a fully passive architecture of a knee prosthesis. Knee flexion close to able-bodied gait is particularly relevant for low-income users of passive prosthetic knees in the developing world, who repeatedly report the need for an inconspicuous gait to mitigate the severe socioeconomic discrimination associated with disability [4,6,9].

6.2 Mechanism Innovation. The combination of the two mechanism modules presented in this article addresses the mechanical limitations of existing passive prosthetic knees designed for low-income users in the developing world. With the advent of active lower limb prostheses in the developed world over the last two decades, many studies in lower limb prosthetics have focused on the optimization of electromechanical systems to achieve better clinical outcomes for users. Over the same time period, only a few innovations have been commercialized in passive, low-cost prosthetics [6–8]. A large proportion of persons living with major lower limb loss in the developing world cannot afford the active prosthetic technology being developed for the high-income, insurance-driven markets of Europe and the Americas.[10] The stability and damping modules presented in this article offer high-performance, passive solutions toward improving walking kinematics, with the eventual goal of mitigating the socioeconomic discrimination, resulting from amputation among low-income users.

This study discusses two novel mechanism applications that were informed by deterministic design principles in the specific context of prosthetic knee design [40]. In the design of the four-bar latch in the stability module, we implemented a quantitative, geometric method to optimize the flexion zone available to above-knee prosthesis users to initiate late stance flexion. In the design of the shear-based damping module with first-order resistive torque, we extended its prior application from other industries to the field of lower-limb prosthetics. Further, we presented a deterministic sizing model and an assembly technique that can enable researchers and designers of passive prosthetic knees to tailor the damping mechanism to specific user needs. Since the damping coefficient is controlled by the number of rotor and stator plates, while the housing, coupler, and other components remain the same, this design can be translated into a low-cost product. In addition, medical devices that require high braking torques in small confined spaces, such as exoskeletons and orthotic braces, could implement the damping mechanism presented in this article. The patent applications filed for these mechanisms lay out the detailed construction and alternative embodiments that may be applied to different contexts [41,42].

Finally, a distinct feature of both the mechanisms is their modular applicability to existing single-axis prosthetic knees. For example, the four-bar latch could be incorporated in existing single-axis knees (Figs. 2(*a*) and 2(*c*)) to improve their stability performance. The 3R80 passive prosthetic knee made by Ottobock uses a conventional rotary hydraulic damper, which may be substituted with the co-axial, rotary damper designed in this study [43].

6.3 Limitations. The flexion zone analysis for the stability module was presented only for level-ground walking, whereas prosthesis users in the developing world often need to navigate uneven terrains [5,44]. A similar analysis could be carried out using able-bodied gait data for walking on slopes and inclines. This could further optimize the location of the virtual locking axis and the corresponding flexion zone.

The presented testing in India is preliminary and should be considered as qualitative proof of the knee performance. The knee flexion data presented are calculated only in two dimensions and does not capture any possible rotation in the frontal plane. In addition, a sensitivity study has to be conducted to characterize the effect of damping changes on the gait of the subject. A quantitative study in a motion capture setting is required to accurately obtain the knee flexion angles and fully describe the performance of the presented knee mechanism.

The structural design of the prototype did not account for the cyclic loading of walking, which could lead to fatigue-induced failure of the four-bar latch prototype. A full fatigue analysis of the mechanism would be required before long term trials, in compliance with the ISO-10328 guidelines for prosthetic devices [45].

A significant future innovation in the damping module could be the addition of an adjustment mechanism to tune the magnitude of damping. Traditional hydraulic cylinders achieve this flexibility by providing adjustment of the orifice diameter between the two fluid chambers [33]. Multiple strategies could be considered to achieve adjustability within the current architecture of the damping module (Fig. 6): (i) changing the separation (t) between the plates, (ii) a retractable key coupling between the rotating plates and the shaft that changes the effective number of plate pairs (n) causing the fluid-shear, and (iii) an additional pumping mechanism to change the amount of fluid available for generating the shear torque. However, implementing these strategies into a compact module remains a significant mechanical design challenge. An innovative adjustment mechanism that does not drastically change

[10]See Note 2.

the rotary damper architecture could enable the adoption of the damping module at scale. It could also drastically reduce the setup time in clinical practice and potentially allow users to tune the damping magnitude based on their comfort.

7 Conclusions

In this study, we presented the design methodology and preliminary validation of two distinct mechanisms relevant to applications in single-axis prosthetic knees.

We presented a novel mechanism in the stability module, which was designed to achieve the dual function of stability during early stance and controlled instability that allows knee flexion during late stance. The mechanism of this module was implemented by a latch mounted on a four-bar linkage with a low and distal virtual locking axis, which widened the flexion zone near the knee while maintaining a narrow flexion zone near the foot. The distal location of the virtual locking axis also minimized the possible hyperextension to within 1 deg. The damping module was implemented with a concentric stack of stationary and rotating pairs of plates shearing thin films of high-viscosity silicone oil. The first-order damping torque was applied co-axially to the knee axis, which provided the required resistance to achieve smooth, able-bodied knee flexion during late stance and swing.

For preliminary user-centric validation, a prototype prosthetic knee with the stability module and two dampers with different magnitudes was tested on a single individual with above-knee amputation in India. The stability module was found to function as expected, enabling smooth stance to swing transition and timely initiation of knee flexion. The dampers also performed satisfactorily, as an increase in the damping magnitude was found to decrease peak knee flexion angle during swing phase. Possible applications and further innovations in existing single-axis prosthetic knees were discussed that can significantly improve the kinematic performance of low-cost, passive prostheses designed for the developing world.

Acknowledgment

We would like to acknowledge Dr. Pooja Mukul and the staff at *Bhagwan Mahaveer Viklang Sahayata Samiti* (BMVSS, also known as, the Jaipur Foot Organization, Jaipur, India) for their partnership in our work. We would like to thank the MIT 2.76 class (Fall 2016) for their initial work towards designing the different prosthetic knee modules. Funding for this study was provided by the the Tata Center for Technology and Design at MIT, the National Science Foundation (Award no. 1653758), and the Indo-US Collaborative Program on Affordable Medical Devices (NIH Project no. 1R03HD092676-01).

Conflict of Interest

There are no conflicts of interest.

Data Availability Statement

The datasets generated and supporting the findings of this article are obtainable from the corresponding author upon reasonable request. The authors attest that all data for this study are included in the paper. Data provided by a third party listed in Acknowledgment.

Appendix: Prosthetic Knee Stability Module Dimensions

Figure 10 and Table 1 present the dimensions of the four-bar linkage that sets the virtual locking axis (VLA) in the stability module. The VLA corresponds to the instantaneous center of rotation of the four-bar linkage. The general process of setting the VLA with respect to the knee axis is presented in Sec. 2.2.1.

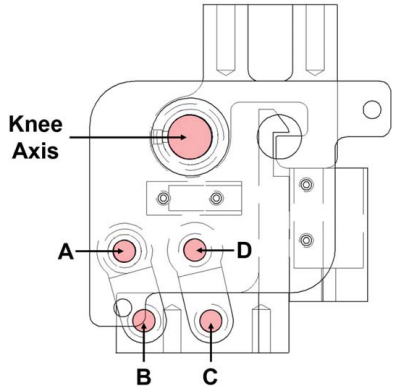

Fig. 10 Technical drawing of the prosthetic knee prototype. Indicated circles show the rotation points in the prosthetic knee prototype. A–D are pivot points of the four-bar linkage that sets the VLA of the stability module. The distance between points A and D is set on the external plate of the knee; the distance between points B and C is set on the latch part of the mechanism. The dimensions between the pivot points are presented in Table 1.

Table 1 Dimensions between pivot points of the four-bar linkage of the stability module

Points	Center-to-center distance (mm)
AB	2.43
BC	1.91
CD	2.43
DA	2.01

Note: The distance is measured between the centers of the corresponding pivot points. For example, AB is the distance between point A and B.

References

[1] World Health Organization, 2011, "World Report on Disability", World Health Organization, Geneva, Technical Report.

[2] McDonald, C. L., Westcott-McCoy, S., Weaver, M. R., Haagsma, J., and Kartin, D., 2021, "Global Prevalence of Traumatic Non-Fatal Limb Amputation," Prosthet. Orthot. Int., **45**(2), pp. 105–114.

[3] World Health Organization, 2017, "World Report on Disability: Standards for Prosthetics and Orthotics," World Health Organization, Geneva, Technical Report.

[4] Narang, Y. S., 2013, "Identification of Design Requirements for a High-Performance, Low-Cost, Passive Prosthetic Knee Through User Analysis and Dynamic Simulation," Master's thesis, Massachusetts Institute of Technology, Cambridge MA.

[5] Narang, I. C., Mathur, B. P., Singh, P., and Jape, V. S., 1984, "Functional Capabilities of Lower Limb Amputees.," Prosthet. Orthot. Int., **8**(1), pp. 43–51.

[6] Hamner, S. R., Narayan, V. G., and Donaldson, K. M., 2013, "Designing for Scale: Development of the ReMotion Knee for Global Emerging Markets," Ann. Biomed. Eng., **41**(9), pp. 1851–1859.

[7] Cummings, D., 1996, "Prosthetics in the Developing World: A Review of the Literature.," Prosthet. Orthot. Int., **20**(1), pp. 51–60.

[8] Andrysek, J., 2010, "Lower-Limb Prosthetic Technologies in the Developing World: A Review of Literature From 1994-2010," Prosthet. Orthot. Int., **34**(4), pp. 378–398.

[9] Mohan, D., 1967, "A Report on Amputees in India," Orthot. Prosthet., **40**(1), pp. 16–32.

[10] Horgan, O., and MacLachlan, M., 2004, "Psychosocial Adjustment to Lower-Limb Amputation: A Review," Disabil. Rehabil., **26**(14–15), pp. 837–850.

[11] Rybarczyk, B., Nyenhuis, D. L., Nicholas, J. J., Cash, S. M., and Kaiser, J., 1995, "Body Image, Perceived Social Stigma, and the Prediction of Psychosocial Adjustment to Leg Amputation.," Rehabil. Psychol., **40**(2), p. 95.

[12] Winter, D. A., 1983, "Energy Generation and Absorption at the Ankle and Knee During Fast, Natural, and Slow Cadences," Clin. Orthop. Relat. Res., **175**, pp. 147–154.

[13] Narang, Y. S., Arelekatti, V. M., and Winter, A. G., 2016, "The Effects of Prosthesis Inertial Properties on Prosthetic Knee Moment and Hip Energetics Required to Achieve Able-Bodied Kinematics," IEEE Trans. Neural Syst. Rehabil. Eng., **24**(7), pp. 754–763.
[14] Narang, Y. S., Arelekatti, V. M., and Winter, A. G., 2016, "The Effects of the Inertial Properties of Above-Knee Prostheses on Optimal Stiffness, Damping, and Engagement Parameters of Passive Prosthetic Knees," J. Biomech. Eng., **138**(12), p. 121002.
[15] Murthy Arelekatti, V., and Winter, A. G., 2018, "Design and Preliminary Field Validation of a Fully Passive Prosthetic Knee Mechanism for Users With Transfemoral Amputation in India," ASME J. Mech. Rob., **10**(3), p. 031007.
[16] Berringer, M. A., Boehmcke, P. J., Fischman, J. Z., Huang, A. Y., Joh, Y., Warner, J. C., Arelekatti, V. N. M., Major, M. J., and Winter, A. G., 2017, "Modular Design of a Passive, Low-Cost Prosthetic Knee Mechanism to Enable Able-Bodied Kinematics for Users With Transfemoral Amputation," ASME 2017 International Design Engineering Technical Conferences and Computers and Information in Engineering Conference, Cleveland, OH, Aug. 6–9 , American Society of Mechanical Engineers, p. V05BT08A028.
[17] Arelekatti, V. M., and Winter, A. G., 2015, "Design of Mechanism and Preliminary Field Validation of Low-Cost, Passive Prosthetic Knee for Users With Transfemoral Amputation in India," ASME 2015 International Design Engineering Technical Conferences and Computers and Information in Engineering Conference, Boston, MA, Aug. 2–5, American Society of Mechanical Engineers, p. V05AT08A043.
[18] Arelekatti, V. M., and Winter, A. G., 2015, "Design of a Fully Passive Prosthetic Knee Mechanism for Transfemoral Amputees in India," 2015 IEEE International Conference on Rehabilitation Robotics (ICORR), Singapore, Aug. 11–14, IEEE, pp. 350–356.
[19] Cavuto, M. L., Chun, M., Kelsall, N., Baranov, K., Durgin, K., Zhou, M., Arelekatti, V. M., and Winter, A. G., 2016, "Design of Mechanism and Preliminary Field Validation of Low-Cost Transfemoral Rotator for Use in the Developing World," ASME 2016 International Design Engineering Technical Conferences and Computers and Information in Engineering Conference, Charlotte, NC, Aug. 21–24, American Society of Mechanical Engineers, p. V05AT07A035.
[20] Gard, S. A., 2016, *The Influence of Prosthetic Knee Joints on Gait*, Springer International Publishing, Cham, pp. 1–24.
[21] Andrysek, J., Klejman, S., Torres-Moreno, R., Heim, W., Steinnagel, B., and Glasford, S., 2011, "Mobility Function of a Prosthetic Knee Joint With An Automatic Stance Phase Lock," Prosthet. Orthot. Int., **35**(2), pp. 163–170.
[22] Winter, D. A., 2009, *Biomechanics and Motor Control of Human Movement*, 4th ed, John Wiley & Sons, Inc., Hoboken, NJ.
[23] Michael, J. W., 1999, "Modern Prosthetic Knee Mechanisms.," Clin. Orthop. Relat. Res. (361), pp. 39–47.
[24] Radcliffe, C. W., 1994, "Four-Bar Linkage Prosthetic Knee Mechanisms: Kinematics, Alignment and Prescription Criteria," Prosthet. Orthot. Int., **18**(3), pp. 159–173.
[25] Wyss, D., 2012, "Evaluation and Design of a Globally Applicable Rear-Locking Prosthetic Knee Mechanism," Master's thesis, University of Toronto, Toronto, Canada
[26] Andrysek, J., Naumann, S., and Cleghorn, W. L., 2006, "Artificial Knee Joint," US Patent 7,087,090.
[27] Smith, D. G., Michael, J. W., and Bowker, J. H., 2004, *Atlas of Amputations and Limb Deficiencies: Surgical, Prosthetic, and Rehabilitation Principles*, 3rd ed., Vol. 3, American Academy of Orthopaedic Surgeons Rosemont, IL.
[28] Furse, A., Cleghorn, W., and Andrysek, J., 2011, "Development of a Low-Technology Prosthetic Swing-Phase Mechanism," J. Med. Biol. Eng., **31**(2), pp. 145–150.
[29] Johansson, J. L., Sherrill, D. M., Riley, P. O., Bonato, P., and Herr, H., 2005, "A Clinical Comparison of Variable-Damping and Mechanically Passive Prosthetic Knee Devices," Am. J. Phys. Med. Rehabil., **84**(8), pp. 563–575.
[30] Radcliffe, C. W., 1977, "The Knud Jansen Lecture: Above-Knee Prosthetics," Prosthet. Orthot. Int., **1**(3), pp. 146–160.
[31] Staros, A., and Murphy, E. F., 1964, "Properties of Fluid Flow Applied to Above-Knee Prostheses," J. Rehabil. Res. Dev., **50**(3), pp. xvi–xvi.
[32] Lewis, E. A., 1965, "Fluid Controlled Knee Mechanisms, Clinical Considerations," Bull. Prosthet. Res., **10**(3), p. 24.
[33] Budynas, R., and Nisbett, K., 2010, *Shigley's Mechanical Engineering Design*, 9th ed., McGraw-Hill Science/Engineering/Math, New York.
[34] Winter, D. A., 1991, *The Biomechanics and Motor Control of Human Gait: Normal, Elderly, and Pathological*, Waterloo Biomechanics, Waterloo, Canada.
[35] Rumsey, R. D., 1969, "Tuned Viscous Vibration Dampers," Aug. 19, US Patent 3,462,136.
[36] Yazid, I. I. M., Mazlan, S. A., Kikuchi, T., Zamzuri, H., and Imaduddin, F., 2014, "Design of Magnetorheological Damper With a Combination of Shear and Squeeze Modes," Mater. Des. (1980–2015), **54**, pp. 87–95.
[37] Herr, H., and Wilkenfeld, A., 2003, "User-Adaptive Control of a Magnetorheological Prosthetic Knee," Ind. Rob.: Int. J., **30**(1), pp. 42–55.
[38] White, F. M., 2016, *Fluid Mechanics*, McGraw-Hill, New York.
[39] Hedrick, T. L., 2008, "Software Techniques for Two- and Three-Dimensional Kinematic Measurements of Biological and Biomimetic Systems," Bioinspiration Biomimetics, **3**(3), p. 034001.
[40] Schmiechen, P., and Slocum, A., 1996, "Analysis of Kinematic Systems: A Generalized Approach," Precis. Eng., **19**(1), pp. 11–18.
[41] Arelekatti, V. N. M., Winter, A. G., and Dorsch, D. S., 2018, "Passive Artificial Knee," US Patent App. 15/571, 027.
[42] Arelekatti, V. N. M., Winter, A. G., Fischman, J. Z., Huang, A. Y., and Joh, Y.,2018, "Locking and Damping Mechanism for a Prosthetic Knee Joint", US Patent App. 16/617,836.
[43] Blumentritt, S., Scherer, H. W., Michael, J. W., and Schmalz, T., 1998, "Transfemoral Amputees Walking on a Rotary Hydraulic Prosthetic Knee Mechanism: A Preliminary Report," JPO: J. Prosthet. Orthot., **10**(3), pp. 61–70.
[44] Mulholland, S. J., and Wyss, U. P., 2001, "Activities of Daily Living in Non-Western Cultures: Range of Motion Requirements for Hip and Knee Joint Implants.," Int. J. Rehabil. Res., **24**(3), pp. 191–198.
[45] International Organization for Standardization, 2006, "Structural Testing of Lower-Limb Prostheses: Requirements and Test Methods," International Organization for Standardization, Technical Report.